JOURNAL OF GEOPHYSICAL RESEARCH, VOL. 99, NO. B10, PAGES 19,741–19,755, OCTOBER 10, 1994

Transdomain thermoremanent magnetization

David J. Dunlop
Geophysics Laboratory, Department of Physics, University of Toronto, Toronto, Ontario, Canada

Andrew J. Newell
Geophysics Program, University of Washington, Seattle

Randolph J. Enkin[1]
Department of Geology and Geophysics, University of Edinburgh, Edinburgh, Scotland

Abstract. Transdomain thermoremanent magnetization (TRM) is produced when thermally activated transitions between different domain structures become blocked during cooling. This paper investigates transdomain remanence in the pseudo-single-domain size range (<1 μm) in magnetite. We use a one-dimensional micromagnetic model of single-domain (SD), two-domain (2D) and three-domain (3D) structures to determine the energies of these states, the energy barriers between them, blocking temperatures for SD↔2D and 2D↔3D transitions, and relaxation times for the resulting TRMs. Energy barriers are very high at 20°C, from 2000kT to >6000kT for SD↔2D transitions. Transdomain viscous remanent magnetization (VRM) will not occur, even on geological timescales, by a one-dimensional excitation such as edge nucleation of a domain wall. Transdomain blocking temperatures, at which energy barriers fall to 25kT-60kT, are ≥553°C for SD↔2D and ≥574°C for 2D↔3D transitions. There are two separate blocking temperatures, e.g. T_B^1 for SD→2D and T_B^2 for 2D→SD transitions. Usually, only the higher of the two has practical significance because the favored (lower energy) state is already 100% populated at this temperature. Our theory is the first to make quantitative predictions of transition paths, relaxation times, and blocking temperatures for transdomain TRM. It is also quite robust. Relaxing the one-dimensional constraint and introducing crystal defects would make it easier to nucleate domains, but energy barriers and blocking temperatures would not be reduced greatly. Our principal conclusion, that only the lowest energy state at blocking is significantly populated, is a fundamental consequence of the Boltzmann statistics of equilibrium states and is unaffected by the details of transitions between states. Grain interactions may be responsible for the multiplicity of states observed in large titanomagnetite grains following replicate TRM experiments.

Introduction

Paleomagnetic records of lithospheric plate motions are made possible by the remarkable stability of remanent magnetization in magnetic mineral grains. In igneous and high-grade metamorphic rocks, the source of magnetic memory is thermoremanent magnetization (TRM) acquired in the direction of the ambient geomagnetic field as grains cool from above the Curie temperature T_c. The work described here advances our physical understanding of how TRM is produced and makes quantitative predictions of its time stability.

Many different magnetic structures are possible below T_c, depending on grain size and shape. In many cases, the atomic moments spontaneously organize themselves into large domains of uniform spin orientation separated by macroscopically narrow walls of changing spin angle (multidomain or MD structure). Very small grains contain only a single domain (SD) with no wall. Grains of intermediate size can support spin vortices and other complex structures [*Schabes and Bertram*, 1988; *Williams and Dunlop*, 1989; *Newell et al.*, 1993].

Stable TRM is acquired in the following way [e.g., *Néel*, 1949]. At temperatures just below T_c, there are frequent large perturbations of a grain's spin structure, leading occasionally to transitions between structures of different types. With cooling, transitions become more difficult, as expressed by a rapidly increasing relaxation time τ. Eventually, decreasing thermal energy and increasing energy barriers between states prevent further transitions. Because τ depends exponentially on temperature T and on T-dependent grain properties, TRM is frozen in quite abruptly at a blocking temperature T_B. At ordinary temperatures, the structure originally blocked at T_B typically has $\tau > 5$ Ga, ensuring stability of the TRM.

SD structures have the highest net moments and also very high stabilities, but they are not the sole source of TRM.

[1]Now at Pacific Geoscience Centre, Geological Survey of Canada, Sidney, British Columbia.

Paper number 94JB01476.
0148-0227/94/94JB-01476$05.00

Most rocks contain volumetrically far more magnetic grains whose equilibrium state is a MD or intermediate structure. Furthermore, grains are not always in their equilibrium state. Other structures of slightly higher energy may also be permitted. These structures are called local energy minimum (LEM) states [*Moon and Merrill*, 1984, 1985].

In this paper, we consider how TRM in an ensemble of grains of a particular size is partitioned among different LEM states. One LEM state can be transformed into another by a transdomain transition. When these transitions become blocked, transdomain TRM [*Moon*, 1985] results.

Néel's [1949] SD theory of TRM deals with rotations of SD moments between states aligned or antialigned with an applied field **H** (SD↔SD′ transitions). Theories of TRM in MD grains [*Néel*, 1955; *Schmidt*, 1973; *Dunlop and Xu*, 1994; *Xu and Dunlop*, 1994] deal with domain wall displacement, which is a relatively low-energy mechanism for transitions between MD magnetization states. Since walls themselves have moments, with two possible orientations depending on the sense of rotation of spins across the wall, one can also imagine TRM in two-domain (2D) grains due to an equilibrium distribution of wall moments and controlled by reversals of these moments (2D↔2D′; see, for example, *Dunlop* [1977]).

Transdomain TRM is more difficult to model because it involves transitions between dissimilar structures and the "path" followed (the set of transitory intermediate states) is not obvious. Experimentally, it has been known for about a decade that the preferred LEM state depends on magnetic history and may be rather different following isothermal hysteresis, alternating field demagnetization, or thermal cycling. But even when a particular grain has a cyclic history, e.g., is repeatedly taken through the same hysteresis loop or is given a series of TRMs under identical conditions, it can exhibit a variety of states [*Halgedahl and Fuller*, 1980, 1983; *Metcalf and Fuller*, 1987; *Heider et al.*, 1988; *Halgedahl*, 1991]. Focussing on TRM in particular, it must be possible to have transitions among the various LEM states at high T and to stabilize a structure other than the equilibrium (or global energy minimum (GEM)) state during cooling.

In this paper, we examine transdomain TRM for SD↔2D and 2D↔3D transitions. By analogy with *Néel's* [1949] treatment of SD↔SD′ transitions, we will assume that each transdomain transition is a first-order thermal activation process, governed by an Arrhenius equation, and that transdomain TRM is a Boltzmann partition among all accessible LEM states, frozen at some T_B to be determined. To make the problem of finding the minimum-energy transition path between LEM states tractable, we use a one-dimensional model of magnetization structure [*Enkin and Dunlop*, 1987]. Such a model can describe the nucleation of Bloch walls at the edge of a particle (longitudinal or edge nucleation [*Dunlop*, 1990; *Halgedahl*, 1991]), but it cannot represent Néel (near-surface) walls or the nucleation of domains and Bloch walls by the propagation of reversely magnetized spikes transversely across a particle (transverse or interior nucleation).

Despite these limitations, a one-dimensional model is a reasonable first approximation. Two- and three-dimensional micromagnetic structures increasingly resemble classic *Kittel* [1949] domain structures as the grain size increases [*Williams and Dunlop*, 1990a; *Newell et al.*, 1993; *Xu et al.*, 1994]. A one-dimensional formulation has the great advantage that only three parameters, the spin angles at either edge of the grain plus the helicity or sense of rotation of the spins, are needed to specify a structure. As a result, we can construct a simplified total energy surface [*Enkin and Dunlop*, 1987] whose topography is easy to visualize. LEM states and the transition paths between them are uniquely defined on the energy surface. Determining the minimum-energy transition path in a multiparameter space, as is required for two- or three-dimensional micromagnetic models, is much more difficult and so far has only been attempted for very small grains with simple SD and vortex structures [*Enkin and Williams*, 1994].

Micromagnetic Model

Following *Enkin and Dunlop* [1987] and *Newell et al.* [1990], each grain was modeled as a rectangular block with x, y, z dimensions L, S, S. For the calculations reported here, the elongation q=L/S was 1.5. The block was subdivided into N=15 layers parallel to the x-y plane. This subdivision was sufficient to resolve the structure of 2D and 3D grains.

Each layer had a uniform magnetization **M**, with $|\mathbf{M}|=M_s(T)$, the spontaneous magnetization of magnetite at temperature T. At room temperature, M_s = 480 kA/m. **M** in a particular layer was in the x-y plane at an angle θ to the x axis. The model is one-dimensional: θ varies only with z, from one layer to another, and not with x and y within a layer. This model is well suited to representing lamellar domains separated by 180° Bloch walls. Because **M** is uniform within each layer and parallel to the boundaries between layers, there are no internal magnetic charges or poles. Pole sheets appear only on the x and y crystal surfaces.

Micromagnetism is a variational approach to finding LEM structures. Starting with a trial structure, i.e., a set of values θ(z), we calculated the sum E_T of exchange, magnetocrystalline, applied field, and demagnetizing energies. The θ(z) were then varied, following an energy minimization algorithm (we used a modified Newton algorithm from the Numerical Algorithms Group library), until further variations did not reduce E_T significantly. Note that a particular LEM structure can be described by only two parameters, the values θ_{left} and θ_{right} of θ in the layers at either edge of the grain. The intervening values of θ are uniquely determined (apart from the sense of rotation, clockwise or counterclockwise) by the minimum energy requirement.

The topography of the total energy surface was mapped by carrying out the same minimization procedure but with θ_{left} and θ_{right} constrained to specific values which were independently stepped through 15° intervals. Very few of these structures are LEM states. They form the grid that allows us to contour the energy surface and visually locate LEM states (lows on the surface) and minimum-energy transition paths crossing saddle points between LEM states. Examples are given in the next section.

We included four contributions to the total energy E_T. The angle-dependent part of the exchange energy is

$$E_{ex} = ALS \int [d\theta(z)/dz]^2 \, dz, \quad (1)$$

A being the exchange constant (1.33×10^{-11} J/m for magnetite [*Heider and Williams*, 1988]). Magnetocrystalline

anisotropy was represented by a uniaxial approximation with θ=0 the axis of easy magnetization:

$$E_a = K_u LS \int \sin^2[\theta(z)]\, dz. \quad (2)$$

The uniaxial anisotropy constant K_u was set equal to the cubic anisotropy constant for magnetite, $|K_1| = 1.36 \times 10^4$ J/m^3. Magnetostatic energy due to an external field **H** applied in the x-y plane at angle β to the x axis is

$$E_h = -\mu_o M_s HLS \int \cos[\beta - \theta(z)]\, dz. \quad (3)$$

E_{ex}, E_a, and E_h are local energies: there is a single contribution from each layer determined by θ in that layer. The demagnetizing energy E_d is nonlocal and requires summing Coulomb interactions between all pairs of pole sheets, including self-energies due to interaction of poles within a sheet:

$$E_d = (\mu_o/4\pi) \iint (\sigma\sigma'/r)\, ds\, ds'. \quad (4)$$

Here ds, ds′ are elements of the x and/or y crystal surfaces with magnetic charge densities σ and σ′, respectively, and r is the distance between the pair of elements. Only the surface charge densities σ, σ′ are varied during the energy minimization. The geometry (i.e., r) is fixed, and so *Rhodes and Rowlands'* [1954] analytic solutions for Coulomb interaction potentials of rectangular charged sheets need only be calculated once. Nevertheless, calculation of E_d used most of the computation time.

Both the total energy E_T and the relative contributions of E_{ex}, E_a, E_h, and E_d to E_T change with heating by virtue of the T dependences of M_s, A and K_u (see *Newell et al.* [1990] for a full discussion). The changes are pronounced near T_c, where M_s drops rapidly to zero. Because $K_u(T)$ decreases as $M_s^{10}(T)$ approximately, the contribution of E_a to the energy budget is negligible above ≈300°C. A(T) decreases as $M_s^{1.7}(T)$ approximately [*Heider and Williams*, 1988]. E_{ex} therefore drops off with heating somewhat less rapidly than E_d, which varies as $M_s^2(T)$. $E_h \propto M_s(T)$ and decreases more slowly than the other energies. Just below T_c, E_{ex} and E_h will dominate the total energy, producing a SD state.

Energy Surfaces and Transition Paths

Figure 1 illustrates typical energy surfaces at and just below T_c, which is 580°C for magnetite. The parameters used were L=0.255 μm, q=1.5, **H**= 100 μT (similar to Earth's field) at angle β=0 (i.e., along the x axis, parallel to the long dimension of the grain). Contour values are E_T normalized to E_{SD}, which is E_d for a SD structure with θ=0 (i.e., **M** parallel to the x axis). "At" 580°C (in reality, 0.1°C below T_c to ensure a nonzero M_s), the only stable structure is SD, with $\theta_{left} = \theta_{right} = 0°$. E_T/E_{SD} values are <1 because $E_h<0$.

The influence of **H** decreases rapidly with falling temperature. By 579°C, the SD energy is about 80% of what it would be for **H**=0. Below 578°C, **H** has little influence on energies or structures, apart from determining preferred directions for domain magnetizations.

By 579°C, a 2D LEM state is beginning to develop, and by 578°C it is the lowest energy or GEM state. The 2D LEM is not exactly at (0°,180°), which is one of the grid points of the constrained minimizations. The physical reason

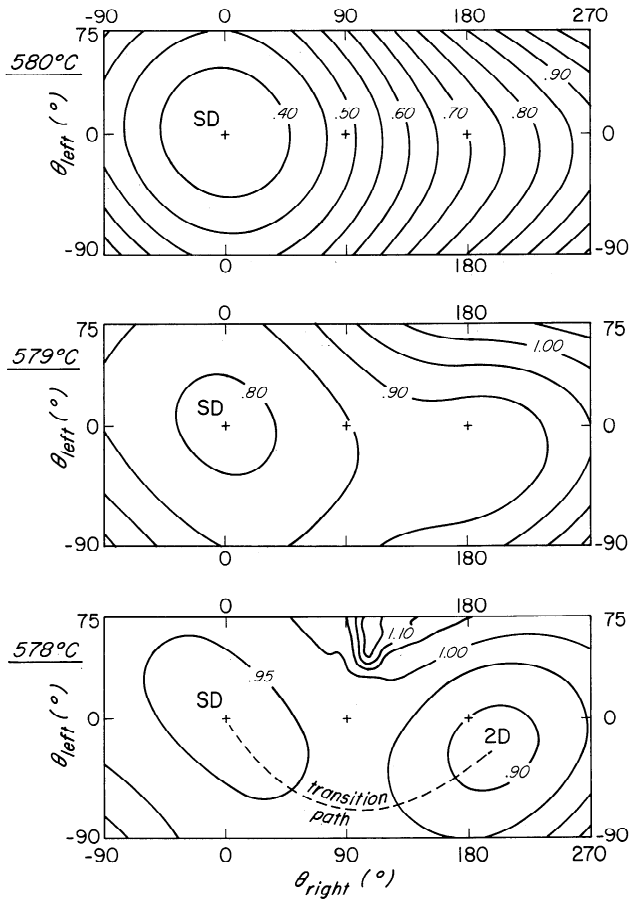

Figure 1. Energy surfaces (contour maps of E_T/E_{SD} for different one-dimensional magnetic structures) just below the Curie temperature for a L=0.255 μm, q=1.5 model magnetite grain in a 100-μT field parallel to the long axis. The angles θ_{left}, θ_{right} are easily visualized by referring to the structures shown in Figure 2. Lows on the surface are LEM states (SD, 2D). The transition path is the least energy route over the saddle point between the SD and 2D LEMs.

for this is "overshooting" of θ beyond the easy directions 0° and 180° to produce "skirts" with moments opposing that of the domain wall [*Moon and Merrill*, 1984; *Enkin and Dunlop*, 1987]. The exact coordinates $(\theta_{left},\theta_{right})$ of the LEM and its structure or configuration (intermediate values of θ) are easily found by doing unconstrained minimizations starting from the (0°,180°) minimum-energy configuration.

The least energy transition path over the saddle point between the SD and 2D LEMs has been sketched in. The exact path can be located uniquely by starting from a series of nearby configurations and doing semiconstrained minimizations, in which θ_{right} is held fixed and θ_{left} and all intermediate θ are varied. The process is analogous to making a set of parallel traverses in a fixed direction to locate the bottom of a valley or mountain pass. By fixing θ_{right} rather than θ_{left}, the "traverses" of the energy surface cross the transition path once only. In the critical region near the saddle point, the traverses cross nearly at right angles (see Figure 1). We can then accurately determine the energy barrier between the SD and 2D LEMs by pinpointing E_{max}, the saddle point energy or value of E_T for the highest-energy structure on the transition path, in closely spaced traverses with small increments of θ_{right}.

SD and 2D LEM Structures and Their Stability Limits

Transdomain TRM is only possible if a grain can support more than one type of LEM state, for example, SD and 2D. Our first task is to determine the ranges of L and q for which different LEMs can coexist. If q=1, this range is negligible, and so we confine our attention to q=1.5. The 2D LEM structures at 20°C and 570°C for a grain with L=0.224 μm and q=1.5 are shown in Figure 2. In both cases, **M** overshoots the easy directions 0° and 180°. The domains are wider and the wall is narrower at 20°C than at 570°C. The reason for this difference is that E_a, which tends to minimize rotations of θ away from the easy axes, is influential at room temperature but negligible at high T.

The existence and coexistence regions at various temperatures for SD and 2D LEMs when q=1.5 are shown in Figure 3. These calculations are for **H**=0, but the results change very little for **H** ≈ the Earth's field (≈60-μT). SD LEM states exist for $L \le d_{SD}^{max}$ (the top curve), 2D states exist for $L \ge d_{2D}^{min}$ (the bottom curve), and both states are possible throughout the hatched region in between. The middle curve, marked d_0, traces values of L for which E_T is equal in the SD and the 2D states. Traditionally, d_0 has been thought of as the critical SD size, on the assumption that the SD structure would transform as soon as its E_T grew larger than E_T for a 2D or other structure. Because of the energy barrier between LEM states, this does not necessarily happen, but we shall see later that d_0 does play a determining role in transdomain TRM.

SD and 2D LEMs are possible alternative states over quite a wide range of grain sizes at room temperature, but the coexistence region narrows to only 0.1 μm above 400°C, where TRM blocking temperatures typically lie. In Figure 4, we analyze the energy budget of 2D states near the three curves in Figure 3. E_a is small at low temperatures and negligible in the TRM blocking range. All energies are larger in small grains near d_{2D}^{min} because the structures are cramped: the wall fills most of the grain and skirts are minimal. In larger grains around d_{SD}^{max}, broad domains develop and walls are narrow relative to the grain size (reducing E_a) with ample skirts to offset their moments (reducing E_d). Above 400°C, the balance between E_d and E_{ex} is constant and similar for grains of all sizes.

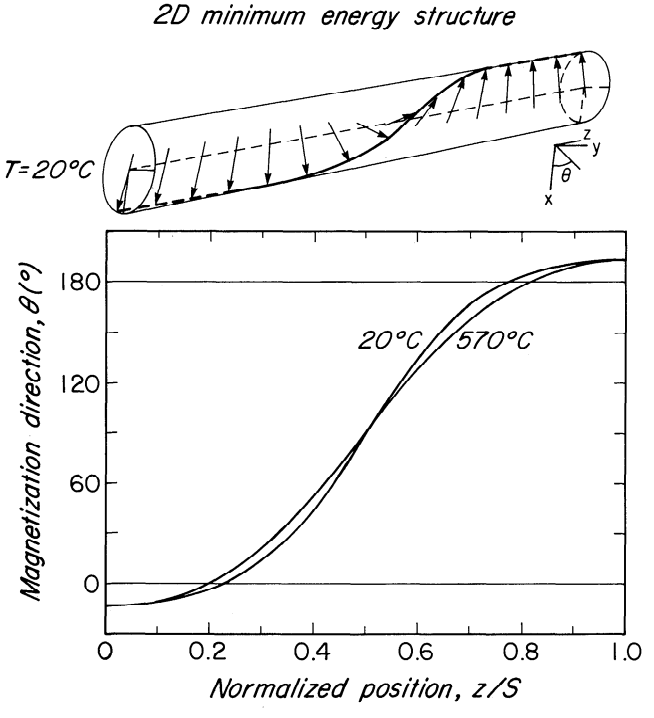

Figure 2. The 2D LEM structures of a L=0.224 μm, q=1.5 magnetite grain at low and high temperatures. The angles θ_{left}, θ_{right} used in the text and in Figure 1 are the values of θ at the left and right edges of the line of spins shown. The "180°" Bloch wall overshoots 0 and 180° but is narrower at 20°C than at 570°C.

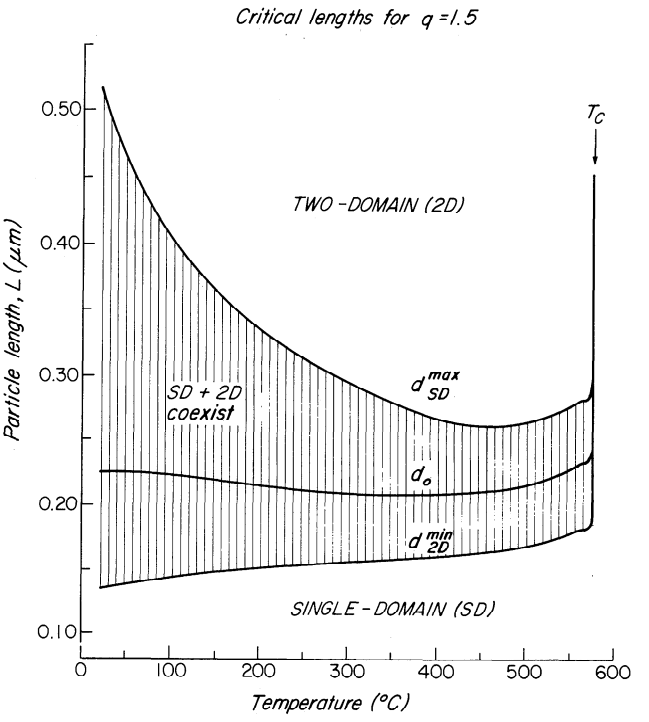

Figure 3. Stability limits for the SD and 2D LEM states in q=1.5 magnetite grains from room temperature to T_c. SD and 2D are possible alternative structures for grains in the hatched region between the minimum 2D size d_{2D}^{min} and the maximum SD size d_{SD}^{max}. Within 1-2°C of T_c, SD is the only possible structure (compare Figure 1). Along the curve labeled d_0, the SD and 2D states have equal total energies.

Transitional Structures

We examined transitory minimum-energy structures along the SD↔2D transition path in L=0.255 μm, q=1.5 grains at 20°C and at 570°C by fixing θ_{right} at angles ranging from 0 (SD state) to 180° (close to the 2D LEM) and doing a semiconstrained minimization of E_T in each case. The energy terms E_a, E_{ex}, E_d, and E_T varied in the way shown in Figure 5. As expected, E_d decreases and E_{ex} increases as the structure is perturbed away from the SD state, but the changes are not smooth. At 20°C, the energies are almost constant until θ_{right} passes 90°. Between 120° and 135°, there are a sharp increase in E_{ex} and corresponding decreases in E_d and E_T. These changes are caused by a rapid change in structure, from one domain with a wall nucleating at the right edge when θ_{right}=120° to a largely complete 2D

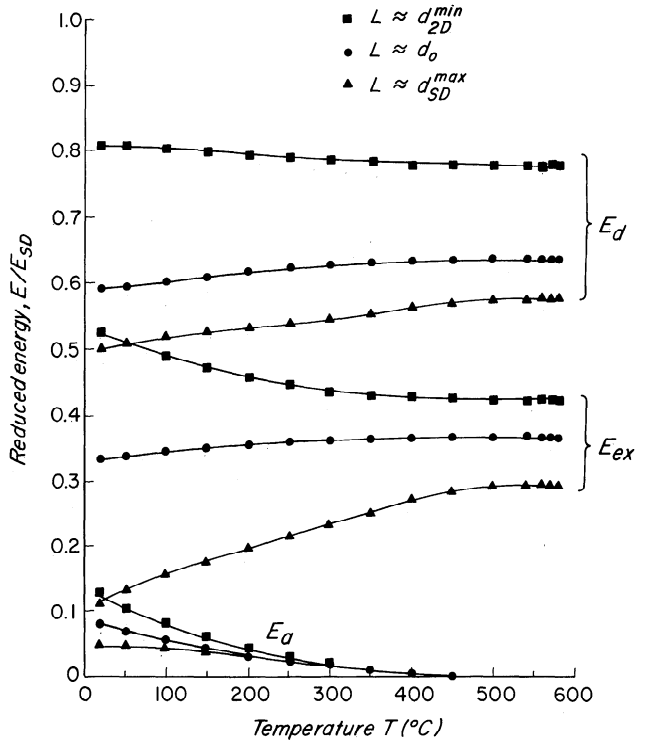

Figure 4. A comparison of energy terms at various temperatures for 2D grains with sizes near the three critical curves in Figure 4. At high temperatures, anisotropy energy E_a vanishes, and the demagnetizing energy E_d is about twice as large as the exchange energy E_{ex}.

structure with a wall in the particle interior when θ_{right}=135° (Figure 6). We have thus pinpointed the onset of edge nucleation as occurring at a specific point along the transition path (just past θ_{right}=120°) and can calculate the exact form of the nucleating structure in whatever detail is desired.

In our treatment of nucleation, we have applied the minimum constraint possible. *Moon and Merrill* [1985], on the other hand, stepped a "virtual wall" of predetermined form across the edge of the grain until it propagated of its own accord, i.e., until E_T began to decrease. We would expect the energy barrier to be lower in our model than in Moon and Merrill's because the wall has freedom to modify its structure so as to reduce E_T. Wall propagation in our model is marked by decreases in all energies at 20°C in Figure 5 between 135° and 180° (and beyond, until the 2D LEM is reached).

At 570°C, the structures are more relaxed (Figure 6) because of the disappearance of E_a and changes in the structures and energies occur more gradually (Figure 5). The saddle point energy E_{max} is also much lower, greatly reducing the SD↔2D energy barrier. These observations suggest that anisotropy, although it is a small energy term at 20°C, may be a determining factor in sharp nucleation. (The situation may be different in high-Ti titanomagnetite where stress-induced anisotropy dominates (B.M. Moskowitz, personal communication, 1994).) Notice that E_T and E_a both peak at θ_{right}=120° when T = 20°C (Figure 5). The change in E_a in this region is small but it is influential because the changes in E_d and E_{ex} more or less balance each other. Qualitatively, the role of E_a is easy to appreciate. Anisotropy tends to rotate moments into the easy directions θ=0 and 180°. It favors the SD structure or a 2D structure with a narrow wall but not intermediate states where the wall is broad.

Energy Barriers at Room Temperature and Transdomain VRM

Plots of E_T versus constrained angle θ_{right} like those of Figure 5 are cross sections through the total energy surface taken along the least energy path between LEM states. This is the most probable transition path, although thermal excitations may cause small deviations from the path during an actual transition. The crucial point on the path is the saddle point, which in Figure 5 occurs near θ_{right}=120°. The difference between the saddle point energy E_{max} and the energy E_{SD} of the SD LEM is the energy barrier E_b which must be overcome to transform the SD structure into a 2D structure by nucleating a Bloch wall at one edge of the grain. If the SD→2D transition is thermally activated, $E_{max}-E_{SD}$ is the activation energy E_{act}. Similarly, $E_{max}-E_{2D}$ is the energy barrier or activation energy for the 2D→SD transition in which the wall "denucleates."

Now let us estimate the relaxation time τ for SD↔2D transitions at ordinary temperatures and assess the likelihood of transdomain viscous remanent magnetization (VRM) [*Moon and Merrill*, 1986]. We will assume that SD↔2D transitions are first-order thermal activation processes described by the Arrhenius-Néel equation:

$$\tau_{ij}^{-1} = C_{ij} \exp(-\Delta E_{ij}/kT). \quad (5)$$

In (5), τ_{ij} is the relaxation time for transitions between states i and j (12 is SD→2D, 21 is 2D→SD), C_{ij} is the rate constant or attempt frequency for individual thermal excitations, ΔE_{ij} is the energy barrier or activation energy $E_{max}-E_i$, where E_i is E_T for LEM state i, and k is Boltzmann's constant. C_{ij} depends on the mode of thermal excitation of the magnetic structure and is thought to be similar ($\approx 10^9$–10^{10} s^{-1}) for SD reversals (SD↔SD′) and MD domain wall activation [*Néel*, 1949; *Brown*, 1963; *Gaunt*, 1977]. Since we require only an order-of-magnitude estimate (C_{ij} being outside the exponential factor in (5)), we will take C_{ij} to be 10^9 s^{-1} for all the transdomain transitions we will consider.

There is a high probability that a particular transition will occur if we wait for a time $t \approx \tau_{ij}$. According to (5), the energy barrier which can typically be surmounted with the help of random thermal impulses in a time t is

$$E_{act} = \Delta E_{ij} = kT \ln(C_{ij}t). \quad (6)$$

If t= 100 s, $E_{act} \approx$ 25kT, and if t= 4.5 Ga (the age of Earth), $E_{act} \approx$ 60kT.

Figure 7 plots E_{act}/kT at 20°C as a function of L for grains with elongation q=1.5. Following *Moon and Merrill* [1986], we assume the grain is initially in its less favored (higher E_T) LEM state and relaxes to the GEM state. This gives the lowest possible energy barrier and is the natural direction for transitions. For $L<d_o$, the GEM state is SD and $E_{act}= \Delta E_{21}$; for $L>d_o$, $E_{act}= \Delta E_{12}$.

Throughout the SD/2D coexistence region (0.15–0.5 μm approximately), E_{act} is between 2000kT and 6300kT at room temperature. Since only ≈25kT of thermal energy is avail-

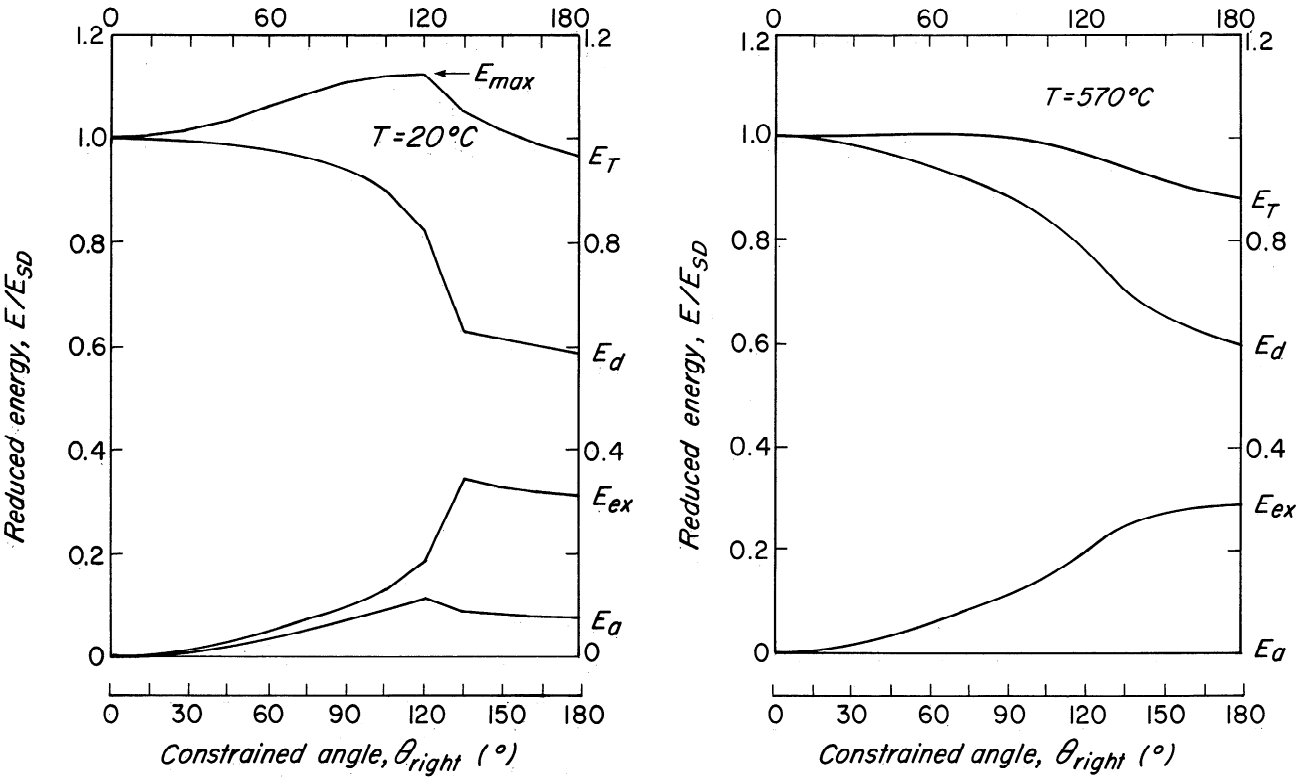

Figure 5. Energy changes accompanying edge nucleation in the model grain of Figure 6. E_d and E_{ex} change most rapidly between θ_{right}= 120° and 135°, but E_a and the total energy E_T peak around 120°, corresponding to the saddle point on the transition path in Figure 1. The saddle point energy E_{max}, which decides the energy barriers that must be overcome in the SD→2D and 2D→SD transitions, is much higher at 20°C than at 570°C.

able on a 100-s timescale and ≈60kT on a 4.5 Ga timescale, transdomain VRM by means of edge nucleation will not occur even on the longest geological timescale. (If t= 4.5 Ga, the probability is exp[−(E_{act}−60kT)/kT] which ranges from e^{-1940} to e^{-6240} and is negligible.) *Moon and Merrill* [1986] implicitly recognized the impossibility of transdomain VRM by a one-dimensional micromagnetic excitation. In their Figure 2, they had to "reduce" their calculated activation energies by factors of ≈1000-2000 to produce any appreciable changes in occupation of LEM states on a 1 Ga timescale.

SD↔2D Energy Cross-Sections at High Temperature

The results of the last section can be viewed in a different light. Since τ_{ij} is >>4.5 Ga at 20°C, a TRM blocked at high temperature and cooled to room temperature will be stable essentially forever. Figure 8 explores how this stability might change with heating, due to either burial in nature or thermal demagnetization in the laboratory, in a 0.21-μm grain.

By heating to 300°C, the energy barrier is approximately halved and the thermal energy (25kT-60kT) is doubled. The transition probability increases (to ≈e^{-1500}) but is still zero for all intents and purposes. Any transdomain remanence can easily survive this heating.

Figure 8 illustrates another way in which stability can change with temperature. Below about 220°C, the GEM state is SD, while above 220°C, the 2D state has lower energy. Now if the grain was originally SD at room temperature, it will remain in a metastable SD state above 220°C because ΔE_{12} is >>60kT up to 300°C (and well beyond). However, if the GEM state spontaneously changes at a temperature high enough that the energy barrier is <60kT, the grain's structure may be thermally excited into the new GEM state given enough time. This is transdomain VRM of a novel type, in which the grain begins in a GEM state, but the GEM state changes with heating. This situation is potentially possible with our model L= 0.21 μm, q=1.5 grain. Above ≈500°C, the GEM state reverts to SD. A horizontal line through L= 0.21 μm crosses the d_0 curve in Figure 3 twice, around 220°C and again around 500°C.

Boltzmann Probabilities and Blocking of SD↔2D Transdomain TRM

Figure 9 traces the blocking process of SD↔2D TRM in L= 0.21 μm, q=1.5 grains. At 574°C, ΔE_{12}= 21kT and ΔE_{21}= 3kT. Both barriers are <25kT, and so, on any normal time scale of observation, thermally excited transitions occur frequently in both directions. In this thermal equilibrium or superparamagnetic condition of rapid transitions, neither LEM state is stable for long enough to preserve a remanence, but the GEM state is much more probable or frequently occupied. The equilibrium Boltzmann probability of each state is

$$p_{eq}^{\,i} = Z^{-1} \exp(-E_i/kT), \quad (7)$$

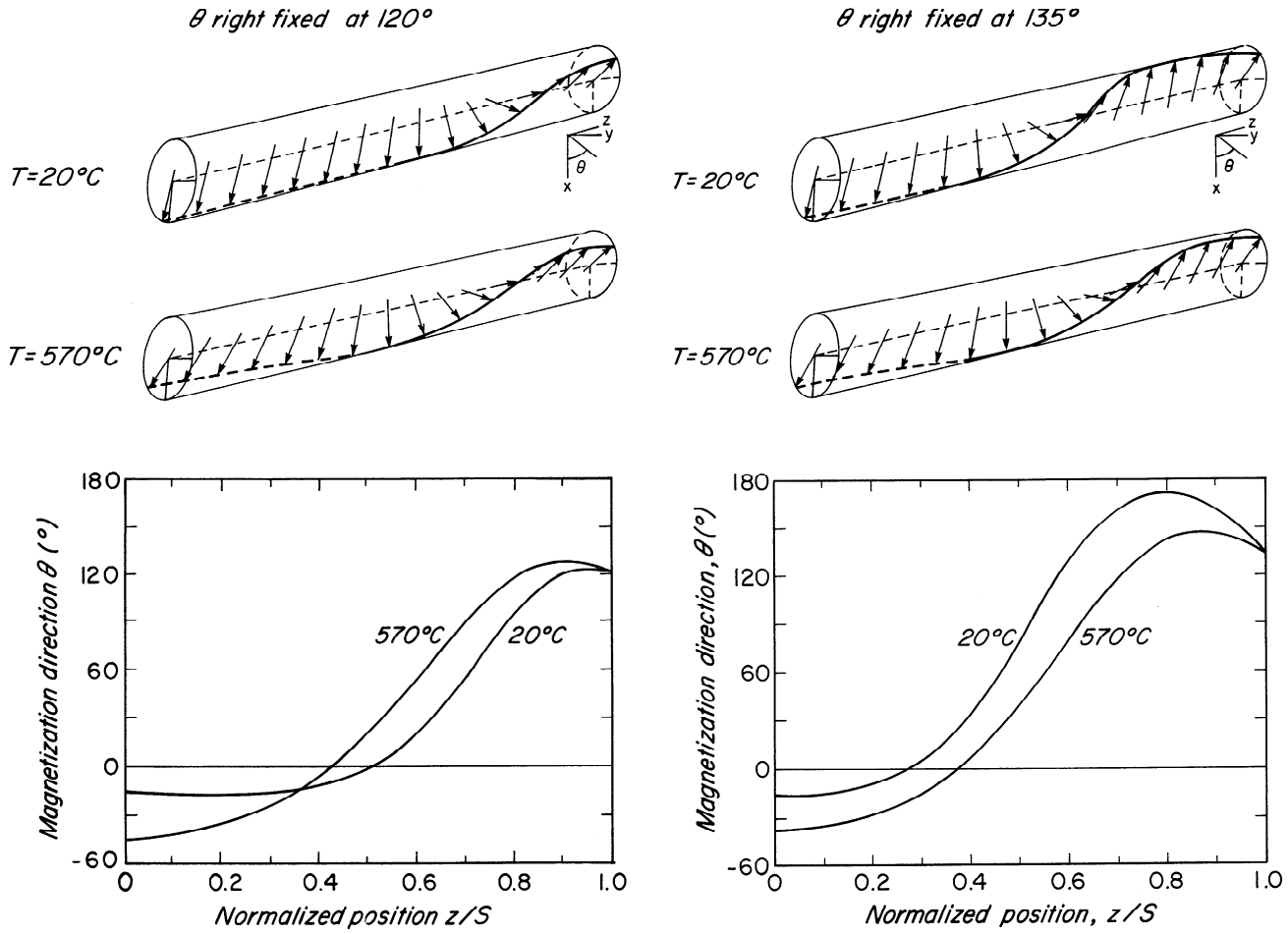

Figure 6. Transitional structures during edge nucleation of a Bloch wall in a L=0.255 μm, q=1.5 magnetite grain. With θ_{right} fixed at 120°, the structure consists of one body domain plus a wall nucleating at the right-hand edge of the grain. By θ_{right}=135°, the wall spontaneously (i.e., with a decrease in E_T) moves into the interior of the grain, generating a second body domain at the right-hand edge.

Z being the partition function or sum of exponential factors over all states. Substituting $E_1=E_{SD}$= 219kT, $E_2=E_{2D}$= 237kT (from Figure 9), we find $p_{eq}^{\ 1}\approx 1$, $p_{eq}^{\ 2}=e^{-18}\approx 0$. Only the SD state is significantly populated in an ensemble of identical grains at any instant. (Actually, SD and SD′ states, with oppositely directed **M** vectors, are about equally populated for small **H**.)

At 570°C, the 2D state is still unstable, but the SD state is stable on laboratory timescales since ΔE_{12} is now >25kT. If **H**→0 at 570°C, the ensemble will preserve a remanence. Even though almost all particles are in the SD GEM state, this remanence is properly called transdomain because the remanence was blocked by quenching SD↔2D transitions. (Note that SD↔SD′ transitions are now also blocked because in grains of this size they can occur only via an intermediate 2D state: SD↔2D↔SD′ [*Enkin and Dunlop*, 1987].)

Just above 560°C, ΔE_{12} increases to 60kT, and transdomain TRM is blocked on geological as well as laboratory timescales. We will call this blocking temperature $T_B^{\ 1}$, because 2D→SD transitions are still possible (ΔE_{21}<60kT). However, the SD occupation probability $p_B^{\ 1}$, which is frozen at the value $p_{eq}^{\ 1}$ at $T_B^{\ 1}$, is ≈1, and there are no 2D structures remaining to be transformed.

Around 540°C, ΔE_{21} reaches 60kT, and 2D→SD transitions are blocked. We call this second lower blocking temperature $T_B^{\ 2}$, but it has no practical significance since the 2D LEM was totally depopulated between $T_B^{\ 1}$ and $T_B^{\ 2}$. This is a general result. At $T_B^{\ 1}$, transdomain TRM is blocked

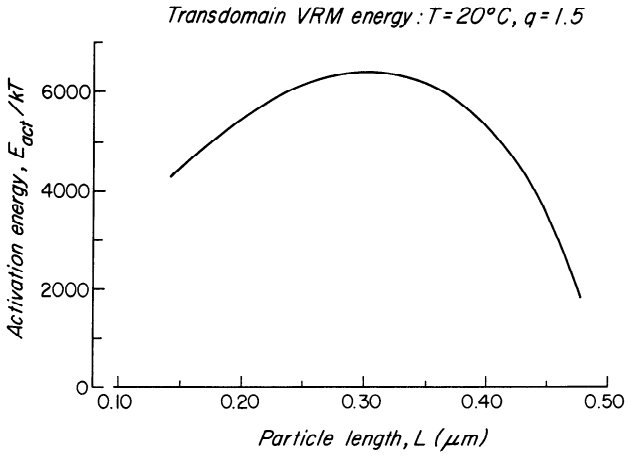

Figure 7. The room temperature activation energy for one-dimensional SD→2D or 2D→SD transitions. An energy of 2000kT to >6000kT is needed to make transdomain VRM [*Moon and Merrill*, 1986] possible, but only 25kT-60kT of thermal energy is available on laboratory to geological timescales.

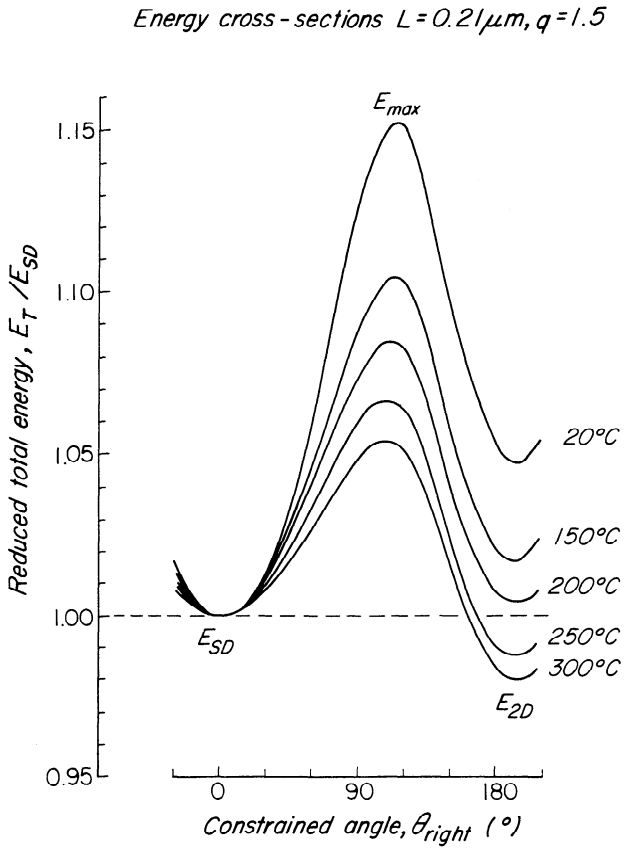

Figure 8. Reduction in SD↔2D energy barriers with heating for a L=0.21 μm, q=1.5 magnetite grain. The energy barrier is approximately halved and the thermal energy is doubled by heating to 300°C, but the probability of a transition remains negligible. Transdomain VRM is insignificant, but transdomain TRM acquired at higher temperatures will be stabilized for times in excess of the age of Earth by cooling to these temperatures.

entirely in the GEM state. Even an energy difference of a few times kT is sufficient to effectively depopulate the less favored LEM state.

As mentioned in the previous section, around 500°C the GEM state changes from SD to 2D (in cooling). The small difference in LEM energies, E_1-E_2= 3kT, which is only one part in a thousand of E_1 or E_2, is sufficient to tip the scales decisively in favor of the new GEM state: $p_{eq}^{\ 2}$=0.977, while $p_{eq}^{\ 1}$=0.023. However, the equilibrium populations cannot be achieved because the 2D GEM state is inaccessible at 500°C: ΔE_{12} is >>60kT. Instead, the SD state remains in metastable equilibrium, with the occupation probability $p_B^{\ 1}$= 1.000 it had at higher temperatures.

Since the d_0 curve in Figure 3 is almost flat until quite high temperatures, there is a very limited range of grain sizes within which transdomain TRM can be blocked in other than the low-temperature GEM state. In fact, this does not occur even for 0.21-μm grains. In Figure 8, we saw that the GEM state reverts to SD in cooling below ≈220°C.

Except within a few degrees of T_c, grains with L=0.23 μm, q=1.5 have 2D GEM states at all temperatures (compare Figure 3). As Figure 10 illustrates, transdomain TRM in this ensemble consists almost exclusively of 2D states and is blocked at $T_B^{\ 2}$≈ 560°C. The lower blocking temperature $T_B^{\ 1}$≈ 540°C, at which transitions out of the (depopulated) SD state are quenched, has no practical importance.

For grain sizes between 0.21 and 0.23 μm, the SD and 2D energies approach each other in the blocking range, and some mixing of states in TRM is possible. Figure 11 illustrates this situation for L= 0.22 μm, q=1.5 grains. $E_b^{\ 1}$ (=ΔE_{12}) opposing SD→2D transitions is only slightly greater than $E_b^{\ 2}$ (=ΔE_{21}) opposing 2D→SD transitions at $T_B^{\ 1}$ (the point where $E_b^{\ 1}$ becomes equal to 60kT, for blocking on a geological timescale, or to 25kT, for blocking on a laboratory timescale). If L is exactly equal to d_0 at the blocking temperature ($T_B^{\ 1}$= $T_B^{\ 2}$ in this case), so that E_{SD}= E_{2D}, equal numbers of SD and 2D states will in principle be blocked. For sizes very slightly above d_0, $T_B^{\ 2}$> $T_B^{\ 1}$ for a 60kT blocking criterion, but $T_B^{\ 1}$> $T_B^{\ 2}$ for a 25kT blocking criterion. It is then possible to block different LEM states on different timescales. Furthermore, in principle, SD TRM blocked around 570°C in rapid cooling would spontaneously revert to 2D TRM if held for geological lengths of time around 550°C.

In practice, mixing and reversion of states are properties of such a limited range of grain sizes that they are little more than interesting curiosities. In the blocking diagram of Figure 12, which plots $T_B^{\ 1}$ and $T_B^{\ 2}$ against L (q=1.5) for both 25kT and 60kT barriers, virtually all TRM in grains plotting to the left of the d_0 versus T curve (taken from Figure 3) is blocked in SD states, since E_{SD}< E_{2D} and ΔE_{12}> ΔE_{21} if L< d_0. Virtually all TRM to the right of the d_0 curve is blocked in 2D states. Only for sizes falling almost exactly on the d_0 curve at blocking should there be any mixing of states in an ensemble of grains, or a choice of LEM states in repeated TRM experiments on a particular grain, as observed experimentally for large titanomagnetite grains [*Halgedahl*, 1991]. The TRM domain state of the vast majority of grains should be predetermined by the exponential Boltzmann probability, which causes a less favored LEM state to be <1% populated if its energy is only a few times kT higher than the GEM state energy. For example, if E_i= E_j+5kT, $p_{eq}^{\ i}/p_{eq}^{\ j}$=exp(−$E_i$/kT)/exp(−$E_j$/kT)=exp[−($E_i$−$E_j$)/kT] = e^{-5} = 0.007.

SD↔2D transdomain TRM has discrete high blocking and unblocking temperatures. All the $T_B^{\ 1}$ and $T_B^{\ 2}$ values in Figure 12 fall in a narrow range between 570 and 575°C for laboratory TRM and thermal demagnetization (25kT barrier) or between 553 and 570°C for very long term heating or slow cooling, due, for example, to deep burial and subsequent erosional uplift (60kT barrier).

Blocking of 2D↔3D Transdomain TRM

Still larger grains can support a three-domain or 3D structure. At room temperature, the coexistence region for 2D and 3D LEM states is quite broad: 0.3 μm ≤ L ≤ 3.0 μm if q=1.5 (Figure 13). There is even a small size range, between L= 0.3 and 0.5 μm at 20°C, in which the hatched areas in Figures 3 and 13 overlap and grains have a choice of three LEM states: SD, 2D, and 3D. This ternary region narrows with heating and disappears above ≈250°C. The 2D + 3D binary region itself narrows to ≈0.3 μm in the TRM blocking range.

As an example, consider TRM blocking in a L= 0.55 μm, q=1.5 grain, which plots close to the d_{2D-3D} curve (Figure 13) along which E_{2D}= E_{3D}. The transdomain energy barriers

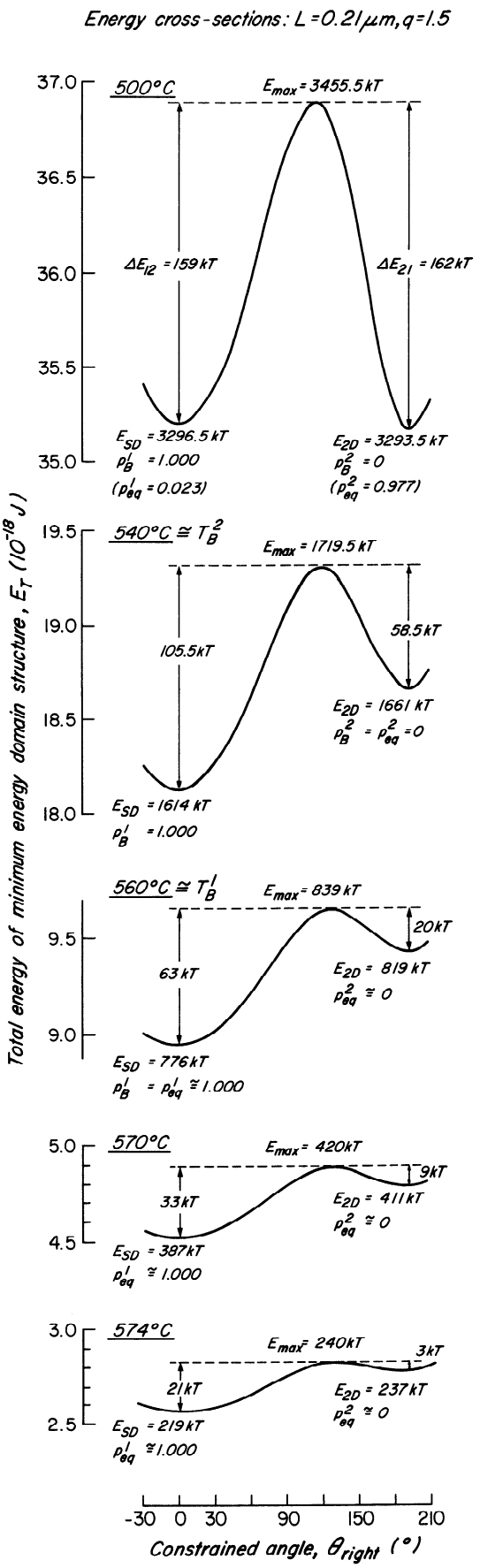

Figure 9. Energy barriers at and above 500°C for transformations between the SD state (θ_{right}=0) and the 2D state (θ_{right}≈190°) in a L=0.21 μm, q=1.5 grain of magnetite. Proceeding from top to bottom simulates thermal demagnetization, from bottom to top simulates TRM acquisition. There are two blocking/unblocking temperatures, T_B^1 and T_B^2 (shown for an assumed 60kT barrier at blocking), corresponding to SD→2D and 2D→SD transitions, respectively. Only the higher of these is significant in practice because below this temperature only the GEM state is populated. The GEM state changes to 2D around 500°C, but the SD state is preserved in metastable equilibrium because the energy barriers have grown >60kT.

ΔE_{23} and ΔE_{32} (Figure 14) are much larger than the barriers ΔE_{12} and ΔE_{21} at the same temperature, mainly because 2D↔3D transitions occur in much larger grains than SD↔2D transitions and the energies scale with the volume of the nucleating or denucleating region (compare equations (1)-(4)). As a result, T_B^3 and T_B^2 for 2D↔3D transitions are >570°C (Figure 15), even higher than SD↔2D blocking temperatures. In L= 0.55 μm grains, 2D is the GEM state down to 576°C but becomes depopulated with less than 1°C of further cooling, when 3D becomes the GEM state (Figures 14 and 15). Transitions out of the 3D state are blocked on a geological timescale just below 575°C, when ΔE_{32} grows larger than 60kT.

Notice that if a 25kT energy barrier is sufficient to produce blocking (laboratory cooling), TRM will be blocked above 578°C in a 2D state (Figure 14). If subsequently held for a long time in a constant field (say during a polarity superchron) at 575°C or so, such a TRM would eventually relax to the now favored 3D GEM state. This is exactly the transdomain VRM process envisaged by *Moon and Merrill* [1986], but the temperatures required to lower the activation energies to ≈60kT and make the process operate are unreasonably high. Under such severe metamorphic conditions, the magnetic minerals would alter and acquire chemical remanent magnetization (CRM).

Despite the apparent choice of two LEM states, grains in the 2D + 3D binary region almost always block in a single, predetermined state. If L< d_{2D-3D} at blocking (i.e., if E_{2D}< E_{3D}), then T_B^2> T_B^3 (Figure 16). The 2D GEM state is blocked and the less favored 3D LEM state is empty. If L> d_{2D-3D} at blocking, as in Figure 15, all the grains carrying TRM are in 3D GEM states. Only for grains very close to d_{crit}= 0.53 μm is there a true choice of 2D or 3D states at blocking (60kT barrier assumed).

Blocking temperatures on a geological timescale range from a low of 574°C for grains around d_{crit} to 578°C for grains near the lower (≈0.4 μm) and upper (≈0.7 μm) 2D + 3D stability limits. On a laboratory timescale, assuming a 25kT barrier, blocking and unblocking temperatures would be even higher. Unblocking temperatures of natural remanence in igneous and metamorphic rocks are seldom this close to T_c. Thus 2D↔3D transdomain TRM due to edge nucleation/denucleation of a domain wall is probably not common in nature.

Discussion

Maximum Size for the SD State

We calculated the maximum size for a stable SD state in moderately elongated magnetite grains (q=1.5) to be d_{SD}^{max}≤ 0.5 μm at room temperature and considerably smaller than this in the blocking range. Experimentally, however, grains

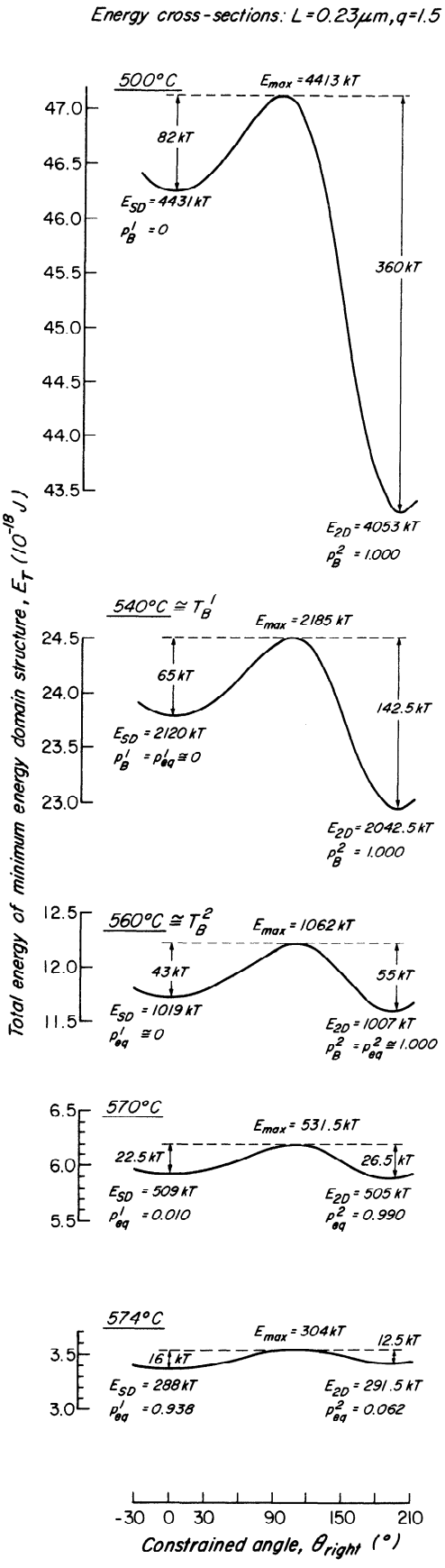

Figure 10. High-temperature energy barriers for SD↔2D transitions in a L=0.23 μm, q=1.5 magnetite grain. In this case, 2D is the GEM state at all temperatures below 574°C and virtually all grains block a 2D TRM in cooling through T_B^2, which is ≈560°C.

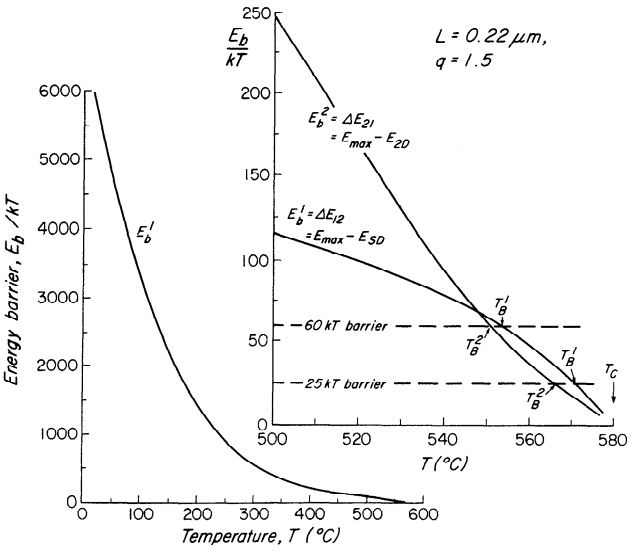

Figure 11. SD→2D and 2D→SD energy barriers and blocking temperatures for a L=0.22 μm, q=1.5 magnetite grain. Because d_0 is close to 0.22 μm in the blocking range, T_B^1 and T_B^2 are quite close to each other, but the Boltzmann probabilities still strongly favor the lower-energy or GEM state, which is SD.

of magnetite and titanomagnetite well above 1 μm in size can remain in metastable SD states following laboratory TRM acquisition [*Halgedahl*, 1991] or thermal cycling [*Boyd et al.*, 1984; *Metcalf and Fuller*, 1987; *Heider et al.*, 1988]. How can we reconcile theory with experiment?

One problem is the one-dimensional constraint built into our model. Two-dimensional calculations [*Xu et al.*, 1994] show that 1-μm magnetite cubes do possess a SD LEM state, which disappears in 5-μm grains. However, the high frequency of SD TRM states observed in titanomagnetite polycrystals by *Halgedahl* [1991] is unexplained. The SD state in 1-μm grains has much higher energy than other LEM states [*Xu et al.*, 1994] and must have a small probability of being occupied during TRM blocking.

Another problem may be our implicit assumption of perfect crystals. Observed metastable SD structures may well contain nuclei of reverse magnetization, but if the nuclei do not develop into full-scale reverse domains, the particle may still image as SD. Crystal defects such as voids, cracks, or surface irregularities generate spikes and closure structures [*Goodenough*, 1954; *Livingston*, 1981], which are frequently observed in large magnetite crystals [*Özdemir and Dunlop*, 1993; Ö. Özdemir et al., manuscript in preparation, 1994]. Our model grains contain no defects and are unlikely to develop nuclei of spikes and closure domains. Another source of reversed nuclei may be spin vortices formed in response to the strong internal demagnetizing fields, e.g., at crystal corners [*Dunlop et al.*, 1990]. Such structures also appear regularly in two- and three-dimensional micromagnetic models of grains near the upper limit of SD stability [*Williams and Dunlop*, 1989, 1990a; *Newell et al.*, 1993; *Xu et al.*, 1994].

Domain Nucleation and Denucleation

The mode of wall nucleation is quite different at low and high temperatures (Figures 5 and 6). At 20°C, the anisotropy energy, although a small term, forces the abrupt nucleation of a relatively narrow wall, whereas at 570°C, the wall is

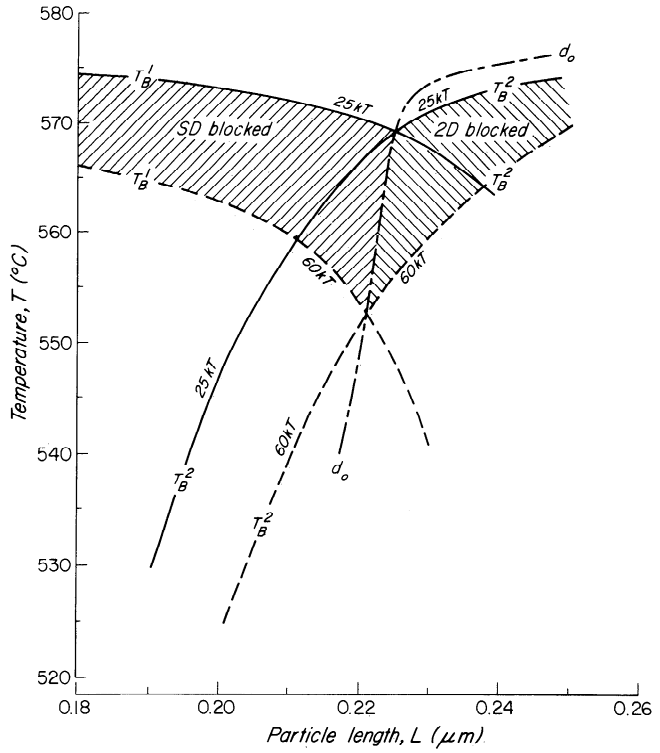

Figure 12. A TRM blocking diagram of T_B^1 and T_B^2 (for SD↔2D transitions) versus grain size. In the entire range between laboratory timescales (25kT blocking barrier) and geological timescales (60kT blocking barrier), only SD states are blocked if $T_B^1 > T_B^2$ and only 2D states are blocked if $T_B^2 > T_B^1$. There is negligible mixing or choice of LEM states at blocking.

wider and nucleates gradually (and much more easily). The only previous theory of edge nucleation [*Moon and Merrill*, 1985] imposed a nucleating wall of fixed form and width. This will lead to overestimates of transdomain barriers, especially in the TRM blocking range.

Edge nucleation leads to high energy barriers, 2000kT to >6000kT, between SD and 2D LEM states at room temperature. A nucleating Bloch wall has a large area, requiring spins to be rotated simultaneously across the entire cross section of the grain, and the new domain will not propagate spontaneously until the wall fills one-third to one-half the grain (Figure 6). Since the energy terms scale with volume, a large energy barrier is inevitable. The barriers are reduced to ≈1000kT-1500kT at 300°C. Since only 25kT-60kT energy barriers can be surmounted with the aid of random thermal fluctuations on timescales ranging from a few minutes to 4.5 Ga, transdomain VRM as proposed by *Moon and Merrill* [1986] is highly improbable.

Near T_c, one-dimensional transdomain transitions become easy and transdomain TRM can be produced. However, blocking/unblocking temperatures are high: ≥553°C for SD↔2D transitions and ≥574°C for 2D↔3D transitions. Although a change in GEM state occurs during cooling for some grain sizes, e.g., for 0.21-μm grains around 500°C and again around 220°C, nucleation or denucleation is prevented by the high energy barriers at these temperatures (≈160kT and >2000kT, respectively, both >60kT).

Experimentally, >1-μm magnetite grains transform from one LEM state to another at temperatures far below T_c by transverse propagation of reverse spikes [*Heider et al.*, 1988]. Spikes often recur at the same location, e.g., at a sharp corner or a surface defect. Future modeling should incorporate reverse nuclei at such sites.

Grain size may be a crucial factor controlling domain structure changes at low and intermediate temperatures (S. Xu, personal communication, 1993). In the <1-μm grains we have modeled, E_d is the dominant energy term and E_a plays a very subsidiary role, even at room temperature (Figures 4 and 5). Since E_d and E_{ex} change in similar ways with T, critical sizes are rather temperature insensitive (Figures 3 and 13) and there is little shift in the LEM state distribution during heating or cooling. In large (>>1 μm) grains, E_a and magnetoelastic (stress-controlled) anisotropy become important. E_a in particular has a strong T dependence and leads to a predicted rapid shift in both the GEM state and the distribution of LEM states with changing temperature [e.g., *Moskowitz and Halgedahl*, 1987]. *Heider et al.* [1988] noted that rapid changes in domain structure in magnetite occurred only in the T range where E_a was changing rapidly; the patterns became irregular (apparently stress-controlled) and temperature insensitive above 200°C.

It is possible that domain state transformations observed far below T_c may not be thermally activated (S. Xu, personal communication, 1993). If the LEM state distribution shifts very strongly in response to the changing balance between E_d, E_{ex}, E_a, and magnetoelastic energy during heating or cooling, some LEM states may disappear and others appear. $E_b \rightarrow 0$ in the process and the structure transforms to an adjacent LEM state with no need for thermal energy. This model is deterministic and does not allow much choice of LEM states in TRM (see next section).

If we assume that most energy barriers between LEM states do not disappear altogether as T changes, there remains a basic problem in finding low-energy paths between

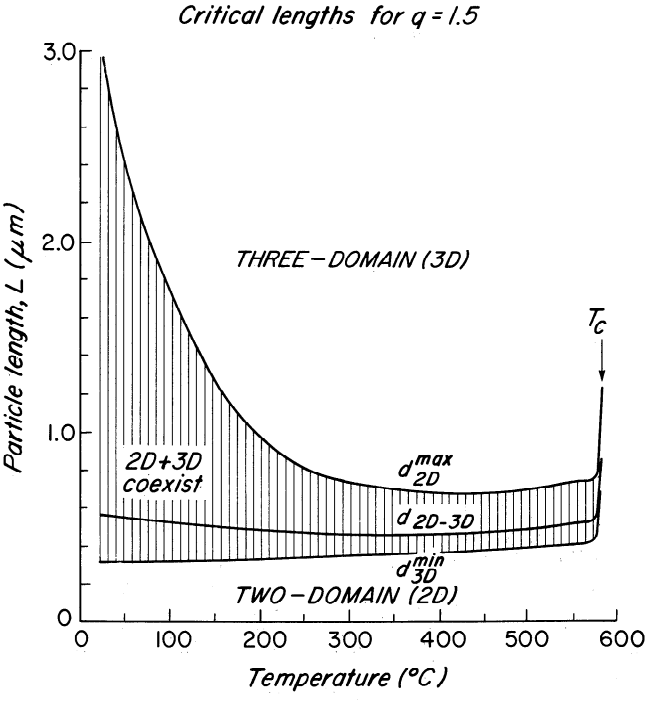

Figure 13. Stability limits for 2D and 3D LEM states. Both states are permitted in the hatched region.

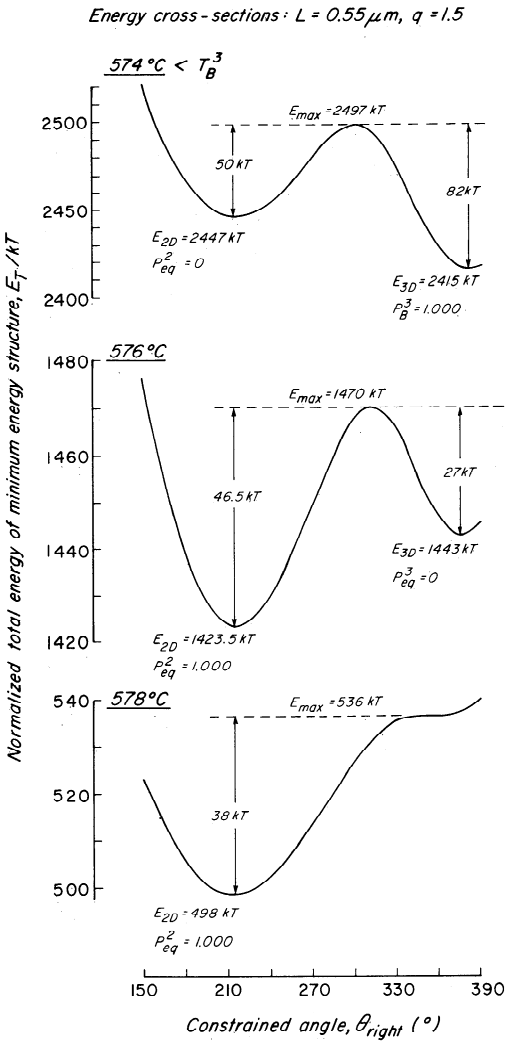

Figure 14. The 2D↔3D energy barriers for a L=0.55 μm, q=1.5 magnetite grain in the range of TRM blocking temperatures. Grains are blocked exclusively in the 3D GEM state at T_B^3, which is just below 575°C on a geological timescale (60kT barrier). The blocking temperatures are much closer to T_c than in the SD↔2D case.

LEM states, however sophisticated the theoretical model used. Energy terms scale with the volume of the nucleating region, and there is an enormous increase in volume between the grains we have modeled and those observed by *Halgedahl* [1991], *Heider et al.* [1988], and *Worm et al.* [1991] among others. For example, although SD is a marginally stable LEM state in a 1-μm magnetite cube [*Xu et al.*, 1994], *Moon and Merrill* [1986, Table 1] found that the "small" energy barrier ΔE_{12} that must be surmounted to transform it to the much lower energy 2D state was (1.866-1.853) × 10^{-14} = 1.3 × 10^{-16} J. At room temperature, this corresponds to 32,000kT, five times higher than our highest room temperature SD↔2D barriers (Figure 7).

A barrier this high could easily preserve metastable SD CRM produced by growth of small grains originally in stable SD states (B.M. Moskowitz, personal communication, 1994). Such a process was modeled by *Newell et al.* [1993]. The same grains (at terminal size) would not preserve a metastable SD state if they were heated to acquire TRM, however.

Multiplicity of LEM States in TRM

We find that the Boltzmann probabilities so overwhelmingly favor the lowest-energy (GEM) state at T_B that there should be no significant mixing of states in TRM. This is a general result, independent of the mineral modeled or simplifying assumptions like one dimensionality and perfect crystals. Energy barriers are not involved (except insofar as they determine the rate of approach to equilibrium), only the LEM state energies. A mere 4kT-5kT energy advantage is sufficient to drain all but the equilibrium or GEM state. For most grains, there is no real choice or partitioning among states; the lowest-energy state is "the" equilibrium state.

Observations by *Halgedahl* [1991], on the other hand, indicate a choice of three or more states in >10-μm titanomagnetite polycrystals. There are no comparable data for >1-μm magnetite grains, but we assume that they also have a choice of LEM states in replicate TRM experiments.

This is not a new problem. In *Néel's* [1949] theory of TRM in SD grains, there are two states (SD and SD′), with moments parallel and antiparallel to **H**. TRM intensity should be proportional to $\tanh[\mu_o V M_s(T_B)H/kT_B]$, which is a Boltzmann partition between SD and SD′ states at T_B. The predicted TRM saturates for small values of H, because the energy of the SD state favored by **H** drops below the SD′ energy until SD becomes the only occupied state. Experimentally, however, TRM saturates rather slowly [*Dunlop*, 1973]. SD′ states must be significantly more populated than predicted.

Dunlop and West [1969] showed that an interaction field $\mathbf{H_{int}}$ added to **H** tips the scales in favor of the SD′ state. A similar model might explain the preservation of less favored LEM states in TRM in *Halgedahl's* [1991] polycrystalline grains. The energy E_i of LEM state i will be lowered (by virtue of E_h) if its net magnetic moment $\mathbf{m_i}$ is closer to the direction of $\mathbf{H} + \mathbf{H_{int}}$ than the moments of competing states. This is quite possible because 2D, 4D, etc., states have net moments due to their Bloch walls, perpendicular to the domain magnetizations [*Stacey and Banerjee*, 1974; *Dunlop*,

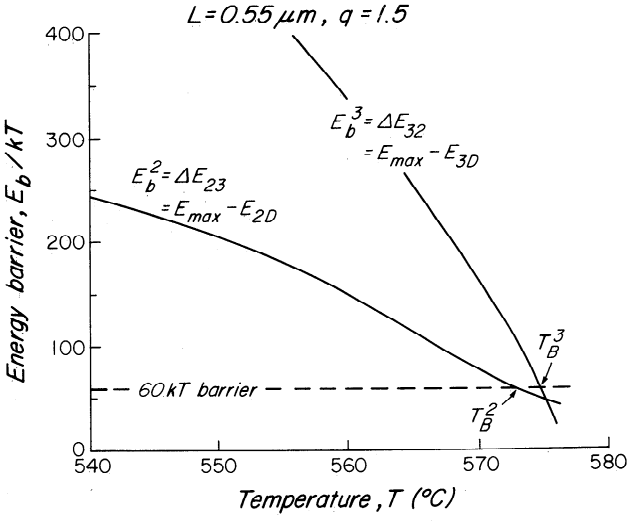

Figure 15. Energy barriers and blocking temperatures for the L=0.55 μm, q=1.5 grain of Figure 14. In this case, the E_b^2 and E_b^3 curves cross between 60kT and 25kT. Thus different GEM states would be blocked in laboratory cooling and very slow cooling in nature.

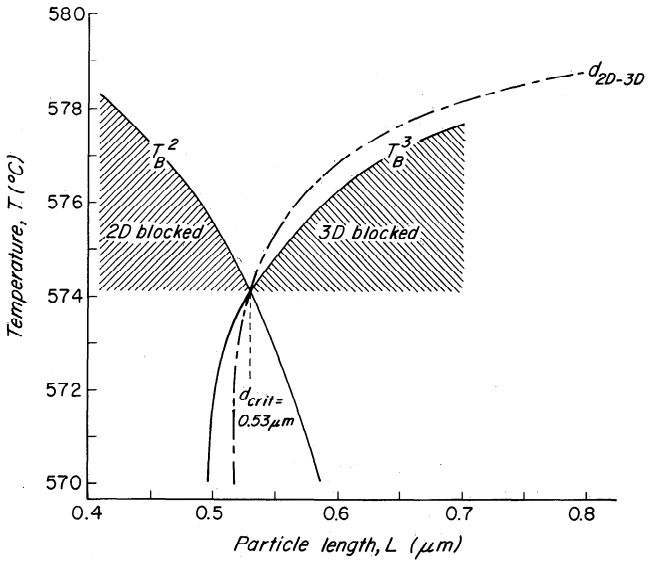

Figure 16. A blocking diagram of T_B^2 and T_B^3 for 2D↔3D transdomain TRM as a function of grain size (only 60kT barriers considered). There is a sharp partitioning into exclusively 2D states in TRM for grains smaller than 0.53 μm and exclusively 3D states for larger grains.

1977], while 3D, 5D, etc., grains have spontaneous moments due to domain imbalance, parallel to the domain magnetizations [*Dunlop*, 1983].

After each heating above T_c, particle interaction fields are regenerated in some new, quasi-random pattern. $\mathbf{H} + \mathbf{H}_{int}$ is in a new orientation and may favor a different LEM state with each new heating and cooling. Edge nucleation is the favored transdomain process in this model because it transforms an odd LEM state (SD, 3D, etc.) into an even state (2D, 4D, etc.) with a perpendicular moment, or vice versa. Transverse nucleation is less favorable because it is an odd↔odd or even↔even transformation and the neighboring LEM states have parallel moments.

Robustness of our Model

Our one-dimensional treatment of edge nucleation of body domains provides the first quantitative physical picture of the transdomain TRM process. In our theory, the transition paths and energy barriers between LEM states are unambiguously defined, an advantage that is lost in two- or three-dimensional micromagnetic models. Nonmicromagnetic transdomain theories [*Moskowitz and Halgedahl*, 1987; *Shcherbakov et al.*, 1993; *Ye and Merrill*, 1994] are heuristic or mathematically based and do not obviously satisfy the basic physical requirements of thermal activation (e.g., the Arrhenius-Néel equation) and Boltzmann statistics.

How much effect would relaxing the one-dimensional constraint have on our conclusions? New LEM structures then appear [*Williams and Dunlop*, 1989, 1990a; *Newell et al.*, 1993] but most are close analogs of one-dimensional SD, 2D, 3D, etc., states. For example, in 0.2-μm magnetite cubes the analog of the uniform SD state is the 1A or flower state [*Schabes and Bertram*, 1988; *Williams and Dunlop*, 1989]. A corresponding SD state is predicted to exist in >1-μm magnetite grains [*Xu et al.*, 1994], but its energy is so high compared to other LEM states that it should occur very infrequently. Thus it is unlikely that relaxing constraints in micromagnetic models can explain the metastable SD states frequently observed in large grains. Probably such structures contain regions of non-uniform magnetization, e.g., vortices or reverse nuclei, which are not imaged.

Transitions between LEM states occur at a rate governed by the height of the energy barrier between the states. A reduction by a factor 2 in energy barriers between SD, 2D, and 3D analog states is possible, but an order-of-magnitude reduction is unlikely. Of course, new transition paths may develop between states. Transverse nucleation is an example. To date, theoretical modeling of alternative modes has only been carried out for "buckling" style vortex reversals between SD and SD′ states. There is at most only a small energy advantage over coherent (one-dimensional) reversals [*Enkin and Williams*, 1994; *Thomson et al.*, 1994].

Halving energy barriers would lower the SD↔2D blocking temperature (using 120kT instead of 60kT barriers in Figures 9-11) by 15-25°C to 530-540°C. The 2D↔3D blocking temperatures would drop even less, from ≈574°C to ≈563°C (compare Figure 15). Equidimensional grains, whose only anisotropy is magnetocrystalline, could in theory have lower energy barriers and blocking temperatures, but they have no choice of LEM states for most temperatures and sizes. Blocking temperatures <500°C are therefore unlikely. Observed domain structure changes just above room temperature cannot be explained by thermal activation.

Why do two- and three-dimensional models achieve only small energy reductions compared to our more constrained one-dimensional model? One reason is that the balance between different energy terms only changes significantly close to T_c and some compensation is possible for small changes. For example, E_d is reduced in our model by skirts flanking domain walls. In two- and three-dimensional models, spin deflections at corners and vortices in the interior of grains serve the same purpose.

The most robust of our conclusions is that only the GEM state should be significantly populated at blocking. This is a consequence of Boltzmann statistics and is almost model-independent. Indeed, reducing the blocking temperature actually tends to increase the dominance of the GEM state.

Finally, all the transdomain blocking temperatures we calculate, or those that are likely with two- or three-dimensional models, are well below the temperature range in which d_o increases to several times its room temperature value (Figure 3). SD structures favored by E_{ex} and E_h within a few degrees of T_c (Figure 1) are not likely to be blocked in large grains and are not a promising explanation of observed metastable SD states in TRM.

To summarize, our one-dimensional micromagnetic model of transdomain TRM is reasonably robust. Our main findings are that: (1) coexistence regions for different LEM states are narrow in the blocking range; (2) critical sizes for different states are temperature insensitive except within 1-2°C of T_c, so that the GEM state at T_B is almost always the GEM state at room temperature; and (3) the energy difference between equilibrium states is comparable to the energy barrier between them, with the result that all states but the GEM state have negligible Boltzmann probabilities when blocking occurs. These findings are robust because findings 1 and 2 depend largely on the T variations of energy terms, which are unchanged in two- or three-dimensional modelling, while finding 3 is independent of the transition path or barrier (although these will determine the exact value of T_B).

Two- or three-dimensional modeling should be attempted, but it is unlikely to substantially lower energy barriers or change our major conclusions. On the other hand, adding reverse nuclei at corners or defects in future modeling might facilitate transdomain transitions below 500°C.

Conclusions

We reach the following conclusions, based on one-dimensional calculations for submicron magnetites.

1. Only over narrow size ranges do small magnetite grains have a choice of states (SD and 2D, or 2D and 3D), especially in the TRM blocking range.

2. SD↔2D transformations by edge nucleation of body domains require large (2000kT–6000kT) activation energies at room temperature. Since only ≤60kT energy barriers can be crossed with the help of thermal fluctuations, even over billions of years, transdomain VRM cannot occur by the mechanism proposed by *Moon and Merrill* [1986].

3. Transdomain energy barriers decrease to 25kT-60kT only at T≥553°C for SD↔2D transitions or T≥574°C for 2D↔3D transitions. Transdomain TRM should have uniformly high blocking and unblocking temperatures.

4. Only the lowest-energy or GEM state has a significant probability of being occupied when TRM is blocked. This is a fundamental consequence of Boltzmann statistics and is not model-dependent.

5. The GEM state can change during cooling but only for very restricted ranges of grain size. Thermally activated transitions to the new GEM state are in any case prevented by the high energy barriers.

6. The predicted determinism of the transdomain TRM state is at odds with the variety of LEM states observed in replicate TRM experiments on large (>10 μm) titanomagnetite grains [*Halgedahl*, 1991]. Grain interaction fields, regenerated in quasi-random fashion in each passage through T_c, may cause different LEM states to be favored in different coolings.

7. Our one-dimensional micromagnetic model is fairly robust. Two- or three-dimensional models may refine our estimates of transdomain energy barriers and blocking temperatures, but they are unlikely to invalidate our conclusions. Future models should incorporate nuclei of reverse magnetization, such as spike domains at surface defects.

Acknowledgments. Discussions about domain structures and nucleation with Song Xu, Özden Özdemir, and Ron Merrill have greatly helped our understanding. Bruce Moskowitz, Lisa Tauxe, and an anonymous referee provided useful reviews. This research was funded by NSERC Research grant A7709 to D.J.D.

References

Boyd, J.R., M. Fuller, and S. Halgedahl, Domain wall nucleation as a controlling factor in the behaviour of fine magnetic particles in rocks, *Geophys. Res. Lett.*, *11*, 193-196, 1984.

Brown, W.F., Thermal fluctuations of a single-domain particle, *Phys. Rev.*, *130*, 1677-1686, 1963.

Dunlop, D.J., Thermoremanent magnetization in submicroscopic magnetite, *J. Geophys. Res.*, *78*, 7602-7613, 1973.

Dunlop, D.J., The hunting of the "psark", *J. Geomagn. Geoelectr.*, *29*, 293-318, 1977.

Dunlop, D.J., On the demagnetizing energy and demagnetizing factor of a multidomain ferromagnetic cube, *Geophys. Res. Lett.*, *10*, 79-82, 1983.

Dunlop, D.J., Developments in rock magnetism, *Rep. Prog. Phys.*, *53*, 707-792, 1990.

Dunlop, D.J., and G.F. West, An experimental evaluation of single domain theories, *Rev. Geophys.*, *7*, 709-757, 1969.

Dunlop, D.J., and S. Xu, Theory of partial thermoremanent magnetization in multidomain grains: I. Repeated identical barriers to wall motion (single microcoercivity), *J. Geophys. Res.*, *99*, 9005-9023, 1994.

Dunlop, D.J., R.J. Enkin, and E. Tjan, Internal field mapping in single-domain and multidomain grains, *J. Geophys. Res.*, *95*, 4561-4577, 1990.

Enkin, R.J., and D.J. Dunlop, A micromagnetic study of pseudo single-domain remanence in magnetite, *J. Geophys. Res.*, *92*, 12,726-12,740, 1987.

Enkin, R.J., and W. Williams, Three-dimensional micromagnetic analysis of stability in fine magnetic grains, *J. Geophys. Res.*, *99*, 611-618, 1994.

Gaunt, P., The frequency constant for thermal activation of a ferromagnetic domain wall, *J. Appl. Phys.*, *48*, 3470-3474, 1977.

Goodenough, J.B., A theory of domain creation and coercive force in polycrystalline ferromagnetics, *Phys. Rev.*, *95*, 917-932, 1954.

Halgedahl, S.L., Magnetic domain patterns observed on synthetic Ti-rich titanomagnetite as a function of temperature and in states of thermoremanent magnetization, *J. Geophys. Res.*, *96*, 3943-3972, 1991.

Halgedahl, S.L., and M. Fuller, Magnetic domain observations of nucleation processes in fine particles of intermediate titanomagnetite, *Nature*, *288*, 70-72, 1980.

Halgedahl, S.L., and M. Fuller, The dependence of magnetic domain structure upon magnetization state with emphasis upon nucleation as a mechanism for pseudosingle domain behaviour, *J. Geophys. Res.*, *88*, 6505-6522, 1983.

Heider, F., and W. Williams, Note on temperature dependence of exchange constant in magnetite, *Geophys. Res. Lett.*, *15*, 184-187, 1988.

Heider, F., S.L. Halgedahl, and D.J. Dunlop, Temperature dependence of magnetic domains in magnetite crystals, *Geophys. Res. Lett.*, *15*, 499-502, 1988.

Kittel, C., Physical theory of ferromagnetic domains, *Rev. Mod. Phys.*, *21*, 541-583, 1949.

Livingston, J.D., A review of coercivity mechanisms, *J. Appl. Phys.*, *52*, 2544-2548, 1981.

Metcalf, M., and M. Fuller, Domain observations of titanomagnetites during hysteresis at elevated temperatures and thermal cycling, *Phys. Earth Planet. Inter.*, *46*, 120-126, 1987.

Moon, T.S., Trans-domain TRM, Ph.D. thesis, 195 pp., Univ. of Wash., Seattle, 1985.

Moon, T.S., and R.T. Merrill, The magnetic moments of non-uniformly magnetized grains, *Phys. Earth Planet. Inter.*, *34*, 186-194, 1984.

Moon, T.S., and R.T. Merrill, Nucleation theory and domain states in multidomain magnetic material, *Phys. Earth Planet. Inter.*, *37*, 214-222, 1985.

Moon, T.S., and R.T. Merrill, A new mechanism for stable viscous remanent magnetization and overprinting during long magnetic polarity intervals, *Geophys. Res. Lett.*, *13*, 737-740, 1986.

Moskowitz, B.M., and S.L. Halgedahl, Theoretical temperature and grain-size dependence of domain state in x = 0.6 titanomagnetite, *J. Geophys. Res.*, *92*, 10,667-10,682, 1987.

Néel, L., Théorie du traînage magnétique des ferromagnétiques en grains fins avec applications aux terres cuites, *Ann. Géophys.*, *5*, 99-136, 1949.

Néel, L., Some theoretical aspects of rock magnetism, *Adv. Phys.*, *4*, 191-242, 1955.

Newell, A.J., D.J. Dunlop, and R.J. Enkin, Temperature dependence of critical sizes, wall widths and moments in two-

domain magnetite grains, *Phys. Earth Planet. Inter.*, *65*, 165-176, 1990.

Newell, A.J., D.J. Dunlop, and W. Williams, A two-dimensional micromagnetic model of magnetizations and fields in magnetite, *J. Geophys. Res.*, *98*, 9533-9549, 1993.

Özdemir, Ö., and D.J. Dunlop, Magnetic domain structures on a natural single crystal of magnetite, *Geophys. Res. Lett.*, *20*, 1835-1838, 1993.

Rhodes, P., and G. Rowlands, Demagnetizing energies of uniformly magnetized rectangular blocks, *Proc. Leeds Philos. Lit. Soc. Sci. Sect.*, *6*, 191-210, 1954.

Schabes, M.E., and H.N. Bertram, Magnetization processes in ferromagnetic cubes, *J. Appl. Phys.*, *64*, 1347-1357, 1988.

Schmidt, V.A., A multi-domain model of thermoremanence, *Earth Planet. Sci. Lett.*, *20*, 440-446, 1973.

Shcherbakov, V.P., E. McClelland, and V.V. Shcherbakova, A model of multidomain thermoremanent magnetization incorporating temperature-variable domain structure, *J. Geophys. Res.*, *98*, 6201-6216, 1993.

Stacey, F.D., and S.K. Banerjee, *The Physical Principles of Rock Magnetism*, 195 pp., Elsevier, New York, 1974.

Thomson, L., R.J. Enkin, and W. Williams, Simulated annealing of three-dimensional micromagnetic structures and simulated thermoremanent magnetization, *J. Geophys. Res.*, *99*, 603-609, 1994.

Williams, W., and D.J. Dunlop, Three-dimensional micromagnetic modelling of ferromagnetic domain structure, *Nature*, *337*, 634-637, 1989.

Williams, W., and D.J. Dunlop, Some effects of grain shape and varying external magnetic field on the magnetic structure of small grains of magnetite, *Phys. Earth Planet. Inter.*, *65*, 1-14, 1990a.

Williams, W., and D.J. Dunlop, Simulation of hysteresis in PSD grains of magnetite (abstract), *Eos Trans. AGU*, *71*, 1289, 1990b.

Worm, H-U., P.J. Ryan and S.K. Banerjee, Domain size, closure domains, and the importance of magnetostriction in magnetite, *Earth Planet. Sci. Lett.*, *102*, 71-78, 1991.

Xu, S., and D.J. Dunlop, Theory of partial thermoremanent magnetization in multidomain grains, 2, Effect of microcoercivity distribution and comparison with experiment, *J. Geophys. Res.*, *99*, 9025-9033, 1994.

Xu, S., D.J. Dunlop, and A.J. Newell, Micromagnetic modeling of two-dimensional domain structures in magnetite, *J. Geophys. Res.*, *99*, 9035-9044, 1994.

Ye, J., and R.T. Merrill, The use of renormalization group theory to explain the large variation of domain states observed in titanomagnetites and implications for paleomagnetism, *J. Geophys. Res.*, *99*, in press, 1994.

D. J. Dunlop, Geophysics Laboratory, Department of Physics, University of Toronto, Toronto, Ontario, Canada M5S 1A7. (e-mail: dunlop@physics.utoronto.ca)

R. J. Enkin, Pacific Geoscience Centre, Geological Survey of Canada, P.O. Box 6000, Sidney, British Columbia, Canada V8L 4B2. (e-mail: enkin@pgc.emr.ca)

A. J. Newell, Geophysics Program AK 50, University of Washington, Seattle, WA 98195. (e-mail: newell@geophys.washington.edu)

(Received January 18, 1994; revised May 23, 1994; accepted June 8, 1994.)